



PERGAMON

Solid State Communications 124 (2002) 83–87

solid
state
communicationswww.elsevier.com/locate/ssc

Raman spectrum and ESR of $\text{Pr}_{0.5}\text{Ca}_{0.4}\text{Sr}_{0.1}\text{MnO}_3$

H.-D. Zhou^a, G. Li^a, F. Liu^a, S.-J. Feng^a, Y. Liu^a, X.-G. Li^{a,*}, J. Fang^b^aStructure Research Laboratory, Department of Materials Science and Engineering, University of Science and Technology of China, Hefei 230026, People's Republic of China^bHigh Magnetic Field Laboratory, Institute of Plasma Physics, Chinese Academy of Science, Hefei 230031, People's Republic of China

Received 9 July 2002; accepted 2 September 2002 by P. Burllet

Abstract

The powder X-ray diffraction patterns, Raman spectra, magnetization, electron spin resonance (ESR), and resistivity for $\text{Pr}_{0.5}\text{Ca}_{0.4}\text{Sr}_{0.1}\text{MnO}_3$ were studied. The Raman spectra change dramatically during the charge ordering transition, and the hardening of the 450 cm^{-1} mode of the spectra is due to the unit cell reduction of the antiferromagnetic phase. The two resonance signals in the first differentiated lines from ESR spectra suggest the coexistence of ferromagnetic and paramagnetic phases above the charge-ordered temperature, which is also confirmed by the insulator–metallic transition above the charge-ordered temperature induced by magnetic fields. © 2002 Elsevier Science Ltd. All rights reserved.

PACS: 75.30.Kz; 75.30.Vn

Keywords: A. Magnetically ordered materials; D. Phase separation; D. Electronic transport

1. Introduction

Recently, many studies about the manganites focus on the coexistence of several magnetic phases, known as phase separation (PS) [1–5]. Particularly, in $\text{Pr}_{0.5}\text{Sr}_{0.5-x}\text{Ca}_x\text{MnO}_3$, the complex competition between ferromagnetic (FM) and antiferromagnetic (AFM) interactions is related to the increase of the bandwidth of the electrons when the Ca atoms are replaced by Sr. $\text{Pr}_{0.5}\text{Sr}_{0.5}\text{MnO}_3$ exhibits an A-type [6] AFM structure with a two-dimensional metallic band and becomes FM metallic at high temperature [7]. In contrast, $\text{Pr}_{0.5}\text{Ca}_{0.5}\text{MnO}_3$ compound is a charge-ordered (CO) insulator with a CE-type AFM spin arrangement [8]. For the intermediate region, Damay et al. [9] have suggested the possibility of the coexistence of the FM and CO phases. The investigations of $\text{Pr}_{0.5}\text{Sr}_{0.41}\text{Ca}_{0.09}\text{MnO}_3$ [10–12] show that it exhibits better magnetoresistance properties than $\text{Pr}_{0.5}\text{Sr}_{0.5}\text{MnO}_3$ and experiences two magnetic transitions from PM to FM then to AFM upon cooling. Furthermore, the evidence of PS within the CO-AFM and FM phases was found in $\text{Pr}_{0.5}\text{Sr}_{0.3}\text{Ca}_{0.2}\text{MnO}_3$ compound by NMR [13]. All

these studies are focused on the PS in CO state with FM phase. However, an important question remains as whether there is FM phase in paramagnetic (PM) state above the charge-ordered transition temperature (T_{CO}) in $\text{Pr}_{0.5}\text{Sr}_{0.5-x}\text{Ca}_x\text{MnO}_3$ system, and further investigation is needed to understand how the lattice varies in the AFM state below T_{CO} .

Electron spin resonance (ESR) has been used to detect the coexistence of different magnetic phases, such as the inhomogeneous paramagnetic state in $\text{La}_{1-x}\text{Ca}_x\text{MnO}_3$ [14] and the PS in $\text{La}_{1.35}\text{Sr}_{1.65}\text{Mn}_2\text{O}_7$ [15]. Raman spectrum has provided valuable information on phonons and other elementary excitations of manganites [16,17], for example the CO and AFM transitions in $\text{Pr}_{0.65}\text{Ca}_{0.35}\text{MnO}_3$ [18].

In this paper, the coexistence of FM and PM phases is found above T_{CO} in $\text{Pr}_{0.5}\text{Ca}_{0.4}\text{Sr}_{0.1}\text{MnO}_3$ by ESR, and the lattice variation in AFM state is studied by powder X-ray diffraction (XRD) patterns and Raman spectra.

2. Experimental

Polycrystalline sample of $\text{Pr}_{0.5}\text{Ca}_{0.4}\text{Sr}_{0.1}\text{MnO}_3$ was

* Corresponding author.

E-mail address: lixg@ustc.edu.cn (X.G. Li).

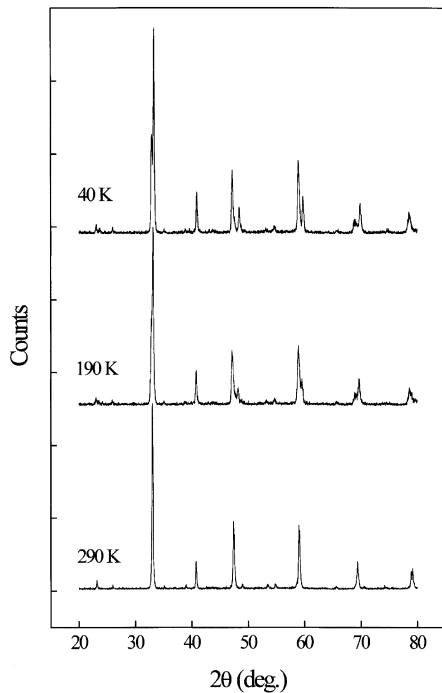


Fig. 1. XRD patterns at 290, 190, and 40 K.

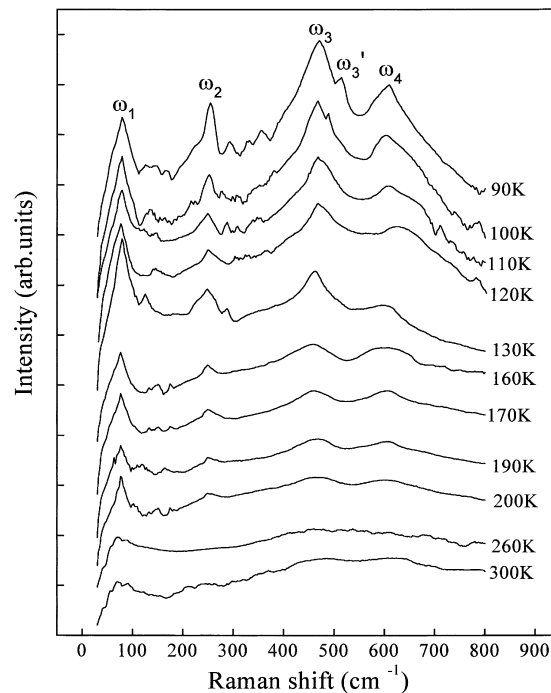


Fig. 3. Raman spectra at different temperatures.

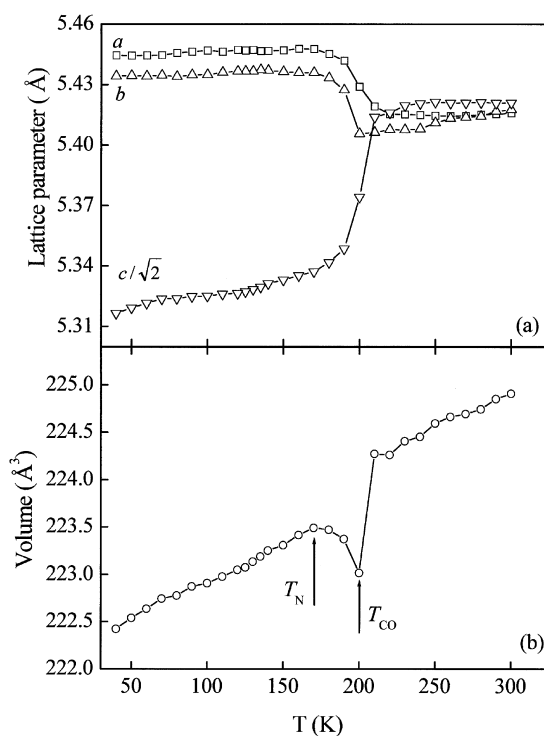


Fig. 2. Temperature dependencies of (a) lattice parameters and (b) unit cell volume.

prepared by a standard solid state reaction method. A stoichiometric mixture of high purity Pr_6O_{11} , SrCO_3 , CaCO_3 , and MnO_2 was ground and calcined in air at 1100°C for 24 h. Afterwards the reactant was reground intermediately and heated at 1200°C for 24 h, then reground, pelletized, and sintered at 1400°C for another 24 h, and was cooled down to room temperature. The powder XRD were recorded by a MacScience MAX-P18AHF diffractometer using $\text{Cu K}\alpha$ radiation. Raman spectra were obtained on a LABRAM-HR Raman spectrophotometer using a back-scattering technique. The ESR measurements were performed at 9.47 GHz using a BRUKER ER-200D spectrometer. The magnetization was measured in a vibrating sample magnetometer (VSM) Ricken Denshi BH55 in a magnetic field of 1000 Gs. The resistivity was measured by a standard four-probe technique at different magnetic fields up to 7 T.

3. Results and discussions

The XRD patterns at different temperatures for $\text{Pr}_{0.5}\text{Ca}_{0.4}\text{Sr}_{0.1}\text{MnO}_3$ are shown in Fig. 1. The characteristic peak of $Pbnm$ space group present at $2\theta = 25.9^\circ$ [7,8] is clearly observable throughout the temperature range from 40 to 300 K. Note that at 190 K some peaks begin to split and at 40 K almost all the peaks split into two peaks, which implies the distortion of the structure at low temperature.

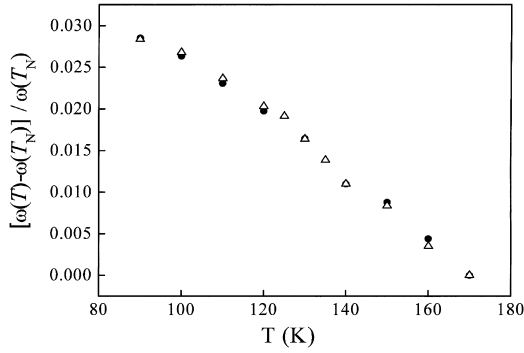


Fig. 4. Temperature dependence of the phonon frequency shift of the ω_3 mode. The solid circles are experimental data and the open circles are the calculated result according to the Grüneisen law.

The temperature dependencies of the lattice parameters, as shown in Fig. 2, indicate the lattice compression along c -axis and expansions along a -axis and b -axis at low temperature. The unit cell volume exhibits a sharp minimum at the charge-ordering temperature T_{CO} (200 K), because Jahn–Teller (JT) distortion via strong electron lattice coupling leads the ‘charge-ordered’ phase accompanied by large changes in Mn–O bond lengths [19,20]. Then a smaller and gradual increase of the unit cell volume was observed at temperature range from 200 to 170 K, which is a common effect of orbital ordering associated with the increasing size of $Mn^{3+}O_6$ octahedral with JT distortion [21]. Below the AFM temperature ($T_N = 170$ K), the unit cell volume decreases monotonously with decreasing temperature.

Fig. 3 shows the Raman spectra excited with 514.5 nm (green) photons at different temperatures. From room temperature down to T_{CO} , a few peaks are clearly observed at about 80 cm^{-1} (ω_1), 450 cm^{-1} (ω_3) and 600 cm^{-1} (ω_4). Below T_{CO} the spectra show dramatic changes, a peak at 245 cm^{-1} (ω_2) becomes clearly visible below T_{CO} , and ω_3 and ω_4 peaks become sharper and gain intensities. At temperature lower than 100 K, a component ω'_3 appears in the spectrum as sideband at slightly higher energy. Polarized

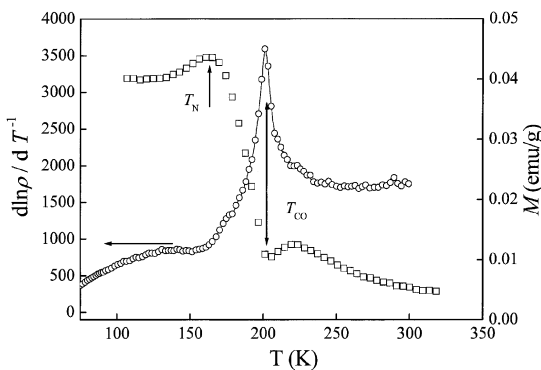


Fig. 5. Magnetization curve (right) and the $d \ln \rho / d T^{-1} \sim T$ curve at zero magnetic field of $\text{Pr}_{0.5}\text{Ca}_{0.4}\text{Sr}_{0.1}\text{MnO}_3$ as functions of temperature. A

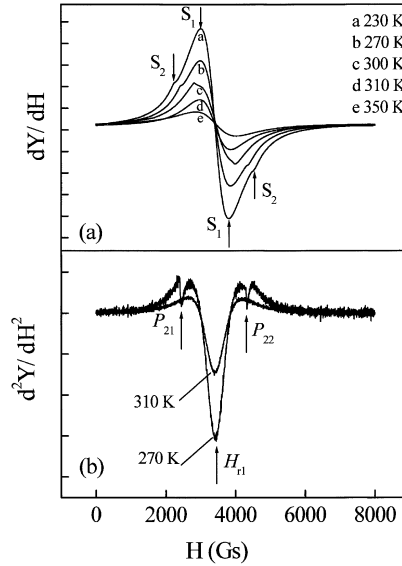


Fig. 6. (a) The first differentiated lines and (b) second differentiated lines for ESR spectra as functions of temperature.

Raman spectroscopy on related compounds assigns ω_2 , ω_3 and ω_4 modes to the oxygen rotation, the apical oxygen bending, and in plane oxygen stretching [22], respectively. The appearance of ω_2 and the peak ‘splitting’ of ω_3 can be explained by the lowering of the symmetry due to JT distortion, which is also confirmed by the splits of the XRD peaks. The intensity increases of ω_3 and ω_4 are due to the formation of the charge-ordered domain which leads a static or quasistatic orthorhombic distortion where the electron hopping rate is strongly decreased [18]. It should be noted that below T_N a slight hardening of ω_3 mode is related to the lattice anomalies or the reduction of the unit cell volume. It is known that optical modes present frequency shifts below the ordering temperature in some AFM and FM transition metal oxides because of magneto and/or exchange stricive effect [23,24]. In our case, the sample shows a quasicubic perovskite structure, reflecting the nearly identical $Mn^{4+}(3t_{2g})\text{--}O(2p)$ bonds for the three binding directions. Therefore one can regard that the Grüneisen law

$$[\omega(T) - \omega(T_N)]/\omega(T_N) = -10.3[V(T) - V(T_N)]/V(T_N)$$

is a good approximation for the lattice contribution to the frequency shift [25], and the calculated result (open triangles) is in good agreement with the experimental data (solid circles), as shown in Fig. 4. This result means that the unit cell volume striction in AFM state dominates the frequency shift of ω_3 mode. This striction is related to the JT effect, since the AFM state can be established only above a certain level of ordering in the mixed $Mn^{3+}\text{--}Mn^{4+}$ system [18].

Fig. 5 shows the variation of magnetization and $d \ln \rho / d T^{-1} \sim T$ curve at zero magnetic field of $\text{Pr}_{0.5}\text{Ca}_{0.4}\text{Sr}_{0.1}\text{MnO}_3$ as functions of temperature. A

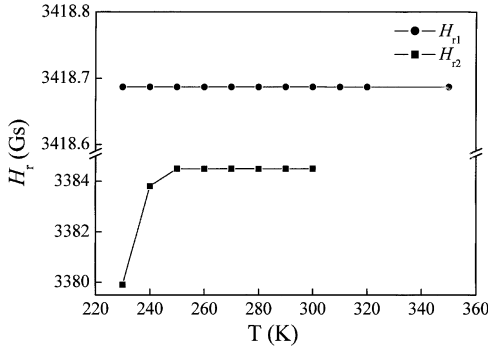


Fig. 7. Temperature dependencies of the resonance field H_{r1} and H_{r2} for S_1 and S_2 , respectively.

minimum in the magnetization curve around 200 K is related to the charge-ordering transition, which corresponds to the peak of the $\ln \rho/dT^{-1} \sim T$ curve. Below charge-ordering temperature T_{CO} (200 K), the value of magnetization begins to drop near 170 K, which coincides with the onset of AFM state. As temperature decreases, the super-exchange interaction competing with double-exchange interaction in the manganites becomes dominant below T_{CO} due to the strong carrier localization, leading to an AFM interaction.

In order to clarify the magnetic nature of $\text{Pr}_{0.5}\text{Ca}_{0.4}\text{Sr}_{0.1}\text{MnO}_3$ more clearly, the electron spin spectra (ESR) are investigated. Fig. 6(a) shows the first differential ESR spectra above 230 K and there are two resonance signals (S_1

and S_2). S_1 has a single Lorentzian shape with unchanged peak position and exists throughout our studied temperature region 230–350 K. S_2 is clearly visible from 230 to 300 K and disappears at higher temperature. In order to define the resonance fields for S_1 and S_2 , we analyze the second differentiation of the ESR spectra. As shown in Fig. 6(b), the resonance field ($H_{r1} = 3418$ Gs) for S_1 keeps unchanged at different temperatures above 230 K, as plotted in Fig. 7. The resonance field for S_2 can be calculated as $H_{r2} = (P_{21} + P_{22})/2$, here P_{21} and P_{22} are the peak positions for S_2 . As plotted in Fig. 7, H_{r2} is smaller than H_{r1} and becomes smaller with decreasing temperature.

According to the resonance condition, the effective resonance field H_{eff} can be described as $H_{\text{eff}} = H_r + H_{\text{int}}$ (H_r is the measured resonance field, H_{int} is the internal magnetic field of the sample). In paramagnetic state, H_{int} is zero and $H_{\text{eff}} = H_r$. If there are some ferromagnetic clusters appearing in the sample, H_{int} will become large and H_r must shift to a lower region in order to keep the resonance, then H_r should be smaller than that of paramagnetic state and it will become more smaller if H_{int} increases with decreasing temperature. These discussions can explain the behaviors of H_{r1} and H_{r2} for S_1 and S_2 , respectively, in our case. So it is proposed that S_1 and S_2 originate from PM state and FM clusters, respectively, which means the coexistence of PM and FM states from 230 to 300 K of $\text{Pr}_{0.5}\text{Ca}_{0.4}\text{Sr}_{0.1}\text{MnO}_3$.

The existence of FM clusters in PM state is also implied by the behavior of resistivity in magnetic fields. Fig. 8 shows the temperature dependencies of resistivity ($\rho \sim T$) and $\ln \rho/dT^{-1} \sim T$ curves in different magnetic fields. With the application of magnetic fields, one can find that (i) when $H > 4$ T there is a metallic region above T_{CO} ; (ii) the peak temperature T_{CO} of the $\ln \rho/dT^{-1} \sim T$ curve shifts to lower temperature, as shown in the inset of Fig. 8(b). The $\ln(\rho/T)$ versus $1/T$ curve, see the inset of Fig. 8(a), shows a linear dependence above T_{CO} at zero magnetic field that suggests polaronic character of the conductivity with hopping energy $E = 160$ meV in the PM state. The suppression of this polaronic character above T_{CO} and appearance of the insulator–metallic (IM) transition in high magnetic fields can be ascribed to the strengthened FM interactions and their percolative properties in the PM state in magnetic fields, which also leads to the decrease of T_{CO} .

4. Conclusion

In summary, in the $\text{Pr}_{0.5}\text{Ca}_{0.4}\text{Sr}_{0.1}\text{MnO}_3$ compound, we observed a hardening of the 450 cm^{-1} mode below T_N in Raman spectra, which is ascribed to the reduction of the unit cell volume according to Grüneisen law. The coexistence of FM and PM phases above T_{CO} is found by ESR measurements. When $H \geq 4$ T, the semiconductor-like region in PM state above T_{CO} can be destroyed to metallic region.

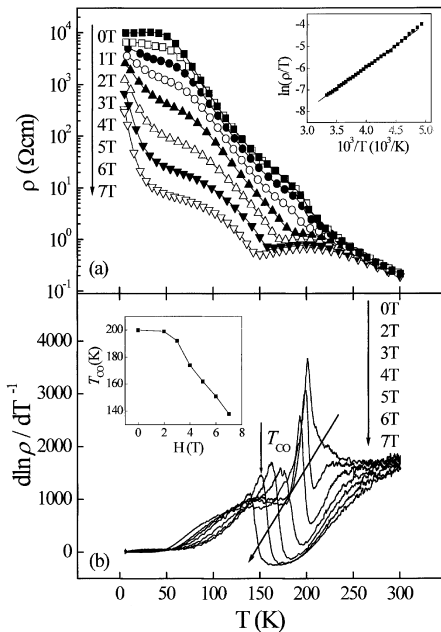


Fig. 8. Temperature dependencies of (a) resistivity and (b) $\ln \rho/dT^{-1} \sim T$ in different magnetic fields. Inset of (a) plot of $\ln(\rho/T)$ versus $1/T$ curve above T_{CO} ; (b) magnetic field dependence of T_{CO} .

Acknowledgements

This work was supported by National Natural Science Foundation of China and the Ministry of Science and Technology of China.

References

- [1] A. Moreo, M. Mary, A. Feiguin, S. Yunoki, E. Dagotto, *Phys. Rev. Lett.* 84 (2000) 5568.
- [2] L. Sudheendra, H.D. Chinh, A.R. Raju, A.K. Raychaudhuri, C.N.R. Rao, *Solid State Commun.* 122 (2002) 53.
- [3] J.H. Dho, W.S. Rim, H.S. Choi, E.O. Chi, N.H. Hur, *J. Phys.: Condens. Matter* 13 (2001) 3655.
- [4] I. Kim, J. Dho, S. Lee, *Phys. Rev. B* 62 (2000) 5674.
- [5] A.K. Raychaudhuri, A. Guha, I. Das, R. Rawat, C.N.R. Rao, *Solid State Commun.* 120 (2001) 120.
- [6] E.O. Wollan, W.C. Koehler, *Phys. Rev.* 100 (1955) 545.
- [7] D. Niebieskikwiat, R.D. Sanchez, *J. Magn. Magn. Mater.* 221 (2000) 285.
- [8] S. Krupicka, M. Marysko, Z. Jirak, J. Hejtmanek, *J. Magn. Magn. Mater.* 206 (1999) 45.
- [9] F. Damay, C. Martin, A. Maignan, M. Hervieu, B. Raveau, Z. Jirak, C. Andre, F. Bouree, *Chem. Mater.* 11 (1999) 536.
- [10] J. Wolfman, C. Simon, M. Hervieu, A. Maignan, B. Raveau, *J. Solid State Chem.* 123 (1996) 413.
- [11] P. Laffez, G.V. Tendeloo, F. Millange, V. Caignaert, M. Hervieu, B. Raveau, *Mater. Res. Bull.* 31 (1996) 905.
- [12] F. Damay, Z. Jirak, M. Hervieu, C. Martin, A. Maignan, B. Raveau, G. Andre, F. Bouree, *J. Magn. Magn. Mater.* 190 (1998) 221.
- [13] M.M. Savosta, A.S. Karnachev, S. Krupicka, J. Hejtmanek, Z. Jirak, M. Marysko, P. Novak, *Phys. Rev. B* 62 (2000) 545.
- [14] S.B. Oseroff, M. Torikachvili, J. Singley, S. Ali, S.W. Cheong, S. Schultz, *Phys. Rev. B* 53 (1996) 6521.
- [15] O. Chauvet, G. Goglio, P. Molinie, B. Corraze, L. Brohan, *Phys. Rev. Lett.* 81 (5) (1998) 1102.
- [16] E. Granado, A.C. Moreno, J. Sanjurjo, C. Rettori, I. Torriani, *Phys. Rev. B* 63 (2001) 064404.
- [17] J.M. Li, C.H.A. Huan, Y.W. Du, F. Duan, Z.X. Shen, *Phys. Rev. B* 63 (2000) 024416.
- [18] V. Dediu, C. Ferdeghini, F.C. Maticotta, P. Nozar, G. Ruani, *Phys. Rev. Lett.* 84 (2000) 4489.
- [19] A.J. Millis, *Nature (London)* 392 (1998) 147.
- [20] P.G. Radaelli, D.E. Cox, M. Marezio, S.W. Cheong, *Phys. Rev. B* 55 (1997) 3015.
- [21] J. Hejtmanek, Z. Jirak, Z. Arnold, M. Marysko, S. Krupicka, C. Martin, F. Damay, *J. Appl. Phys.* 83 (1998) 7204.
- [22] M.N. Iliev, M.V. Abrashev, H.G. Lee, V.N. Popov, Y.Y. Sun, C. Thomsen, R.L. Meng, C.W. Chu, *Phys. Rev. B* 57 (1998) 2872.
- [23] M. Udagawa, K. Kohn, N. Kashizuka, T. Tsushima, *Solid State Commun.* 16 (1975) 779.
- [24] K.H. Kim, J.Y. Gu, H.S. Choi, G.W. Park, T.W. Noh, *Phys. Rev. Lett.* 77 (1996) 1877.
- [25] E. Granado, N.O. Moreno, H. Martinho, A. Garcia, J.A. Sanjurjo, I. Torriani, C. Rettori, J.I. Neumeier, S.B. Oseroff, *Phys. Rev. Lett.* 86 (2001) 5385.